CCUS: 4014768

Re-assessment and Simulation of the Illinois Basin Decatur Project: Integration of New Geological Insights into the Carbon Capture and Storage Evaluation

Juan C. Mejía Fragoso[1], Nicolás Córdoba Castillo[1], Beatriz K. Herrera Hernández*[1], Juan Carlos Gutiérrez B.[1], María A. Santos González[1], Anngy D. Román Ortega[1], Stefany G. Peñaranda González[1], Rocío Bernal-Olaya[1], 1. Universidad Industrial de Santander.

Abstract

The Illinois Basin Decatur Project (IBDP) pilot carbon capture and storage project is the subject of a comprehensive re-assessment. The primary objective is to integrate newly interpreted geological data, including horizons, faults, channels, and bars, into the existing static model; and discuss potential impacts. A refined understanding of the reservoir's architecture and a 3D injection simulation are pursued.

Key activities, including seismic and geological data interpretation, petrophysical analysis, geomechanical characterization, and the critical assessment of fracture pressures, have been employed. These activities have allowed the derivation of an updated static model that includes previously uninterpreted channels and bars as geobodies. This enhanced model forms the basis for 3D injection simulations.

Geological re-assessment of the reservoir shows segments of normal inverted faults that cut through it. More significantly, the interpretation of geobodies as pointbars in a fluvial environment due to the apparent lateral acretion observed in semblance volumes and the lateral property variations observed in the petrophysical analysis, improves the understanding of reservoir structure and character for simulation. The incorporation of new trends of previously uninterpreted channels and bars has added depth and complexity to our static model; as a result, the confidence in simulating the injection process has been enhanced, with the lateral complexity of the reservoir now playing a significant role in modifying connectivity for injection.

The geomechanical process was achieved by using previous sonic and density log analysis to calculate the vertical pressure, pore pressure, horizontal stresses, fracture pressure, and collapse pressure, to determine a

normal stress regime for the area of review (AOR). Fault data taken from the static model identified six faults that cut the Mt. Simon formation. The faults were evaluated in the FSP software (Stanford University) indicating that the faults are stable and unlikely to become flow channels, “thief zones” for injected fluids.

The CO_2 injection simulation contrasted a simplified model with homogeneous, isotropic properties against a more complex and heterogeneous representation that mirrors actual reservoir conditions. This study underscores the significant impact of porosity and permeability variations on the CO_2 plume's shape and movement. It demonstrates that incorporating detailed geological features, such as reservoir heterogeneities, faults, and geobodies, leads to a more accurate definition of the storage area, essential for the secure subsurface sequestration of CO_2.

Introduction

The Illinois Basin Decatur Project (IBDP) is a collaborative project led by the Illinois State Geological Survey (ISGS) at the University of Illinois, along with key partners such as Archer Daniels Midland Company (ADM) and Schlumberger Projeo Corporation, set out to demonstrate the feasibility and effectiveness of large-scale CO_2 sequestration in a deep saline reservoir, the Mt. Simon Sandstone (Brown, 2008). Commencing in 2011, the project successfully injected one million tons of CO_2 by November 2014, a significant achievement in demonstrating the practicality of CCS at large scale (Freiburg, 2014).

Following the IBDP, the Illinois Industrial Carbon Capture and Storage (ICCS) project, also on the ADM property, furthered this initiative by injecting over 1.7 million tons of CO_2 as of March 2020. The primary objective of both projects was to validate the technologies and methodologies necessary for safe, large-volume CO_2 storage in saline reservoirs, a critical component in the global effort to mitigate climate change effects (Zaluski & Lee, 2021).

A distinctive feature of the IBDP and ICCS projects was the continual development and refinement of their geological models and CO_2 injection simulations. This process evolved from early models using basic data in 2008 to highly sophisticated, data-rich models by 2023. The approach included integrating seismic surveys, well logs and time-lapse seismic data to enhance the understanding of the reservoir's structural and petrophysical properties. The final model, completed in 2020 by Zaluski & Lee (op. cit.), was pivotal in accurately simulating CO_2 migration and informed key decisions regarding the project's implementation.

In this paper we propose a geological re-assessment, conducted under the guidance of the SEG EVOLVE 2024 program and its mentors. Our approach encompasses seismic interpretation, petrophysical and geomechanical analyses, static modeling and a conceptual simulation of CO_2 injection to evaluate the injectivity of the reservoir and possible implications into the Illinois Basin Decatur Project (IBDP), thereby contributing to a deeper understanding of the project's potential and challenges in CO2 sequestration.

Geological Context

The Illinois Basin Decatur Project (IBDP) is located within the Illinois Basin, a region with geological interest due to its complex history and stratigraphy (Figure 1). Originating as a failed rift during the late Precambrian, the Illinois Basin evolved into a broad cratonic basin by the late Cambrian, accumulating approximately 100,000 cubic miles of carbonate and siliciclastic rocks through episodic subsidence (Swann, 1968).

Illinois basin primarily consists of Paleozoic sedimentary rocks, aged between 280 to 530 million years, which rest upon an even older foundation of igneous and metamorphic rocks, estimated to be around 1.3 billion years old (Swann, 1968). The Southwest edge of the basin is overlapped by Mesozoic and Cenozoic sediments 90 to 50 million years old.

The study focused on the Cambrian-age Mount Simon Formation, the reservoir for the IBDP and the ICCS, characterized by a thick succession of sandstones, conglomerates and minor siltstones and mudstones. The

Mt. Simon is divided into three major sections (Lower, Middle, and Upper) based on unconformities, and changes in depositional environments including fluvial, eolian, and marine (Freiburg, 2014). Fluvial and eolian deposits occur in both the Lower and Middle and are very similar depositional sequences, however, the best reservoir quality occurs in the Lower Mt Simon Sandstone with an average porosity of 22% and permeability of 200 mD.

The Mt. Simon is overlain by numerous tight formations that act as sealing formations, including the Cambrian Eau Claire, the Ordovician Maquoketa, and the Devonian New Albany, being Eau Clare the primary caprock, which presents two lithostratigraphic components: Siliciclastic dominant lower component and Mixed siliciclastic/carbonate upper component (Leetaru & Freiburg, 2014). Below the Mt Simon is a sandstone unit named Argenta that is known for its poor reservoir quality.

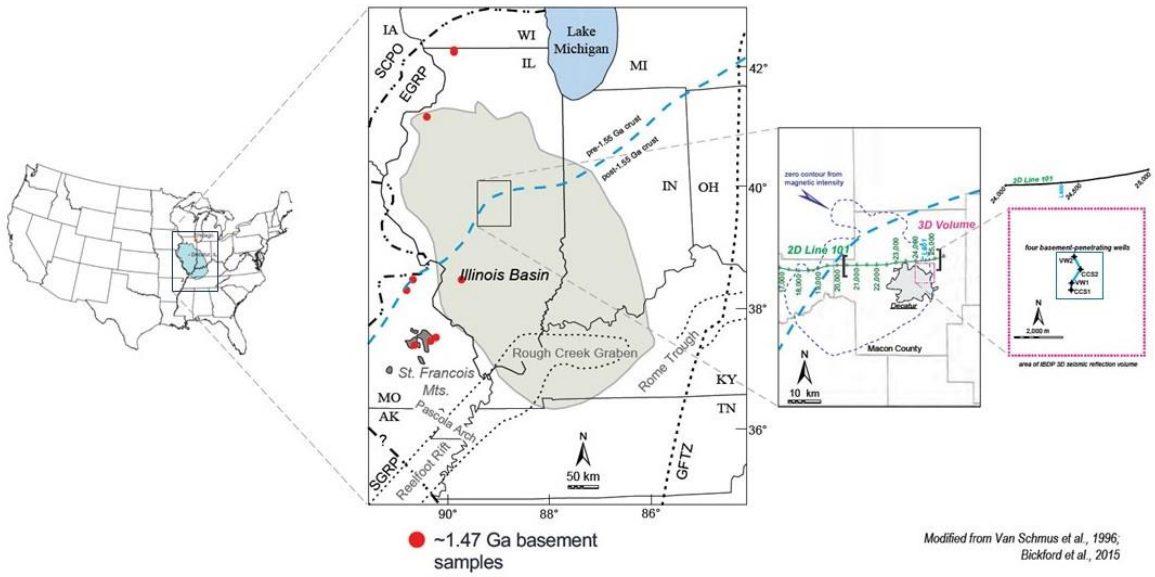

Figure 1. Location of the Illinois Basin Decatur Project, the blue box shows the seismic cube extent. Modified from Freiburg et al., 2020.

Methodology

The re-evaluation of the Illinois Basin Decatur Project involved collecting diverse datasets essential for subsurface analysis from ISGS (2023) and USDOE Office of Fossil Energy (2021). Geographic Information System (GIS) data provided spatial context, while seismic data offered insights into subsurface structures. Well logs contributed to understanding the physical properties of formations. Additionally, original horizon data were crucial for geological and geophysical analyses, enabling a comprehensive evaluation of the study area.

Seismic Interpretation: The seismic interpretation was performed in a 3D seismic cube in depth, provided by ISGS (2023) that consist of 268 inlines and 2992 crosslines with an increment of 40 ft and 5 ft respectively; and a depth of 29000 ft. The reinterpretation of horizons and faults involved a comprehensive analysis of seismic data and well tops. Eau Claire, Mt. Simon and Argenta were manually interpreted based on seismic data and well tops, while inner Mt. Simon and inner Eau Claire were computed with the *Horizon Cube tool* in OpendTect, which incorporated steering data and inputs derived from manually interpreted horizons. The visual representation of the resulting horizons is presented in Figure 2.

In conjunction with horizon interpretation, fault analysis encompassed the utilization of similarity, semblance, and seismic reflectors, revealing a total of six normal inverted faults (Figure 3) Following the reinterpretation of horizons and faults, geobodies were extracted from the RMS amplitude attribute of the

seismic data, using the Geobody Extractor Tool in Petrel within the reservoir zone. 8 geobodies were extracted, they demonstrate an east-west trend, a characterization rooted in the depositional environment; the bodies were defined as sand facies and converted to grid cells to add them to the model later on (Figure 3).

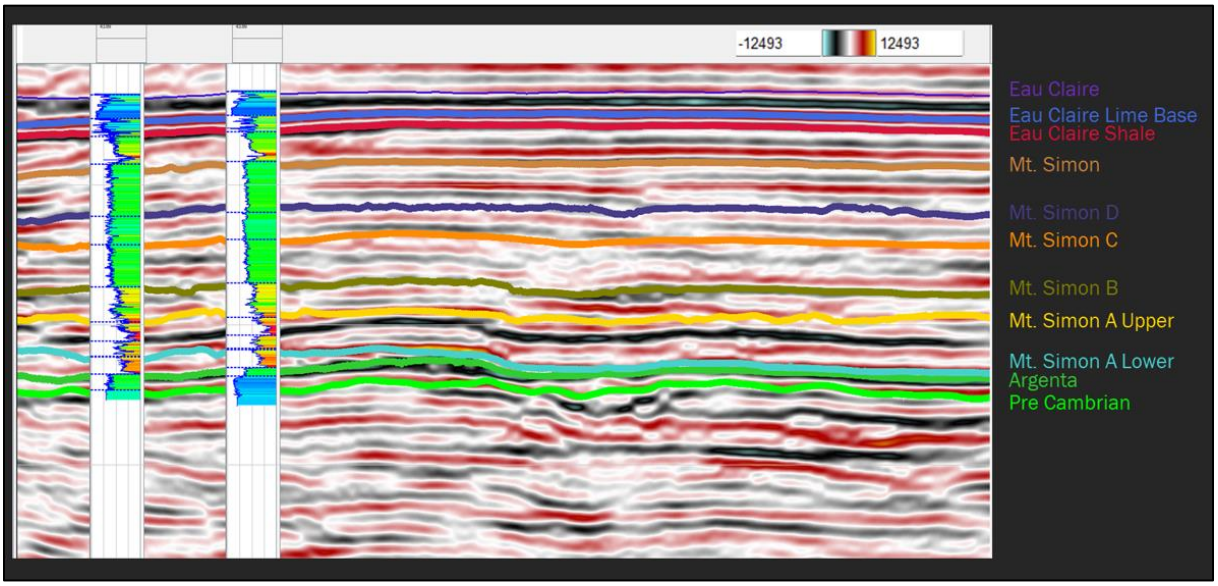

Figure 2. Cross section showing horizons, wells and seismic data along Inline 95, horizontal extent is 800-2800 crossline, depth extend is 4000-8000 ft.

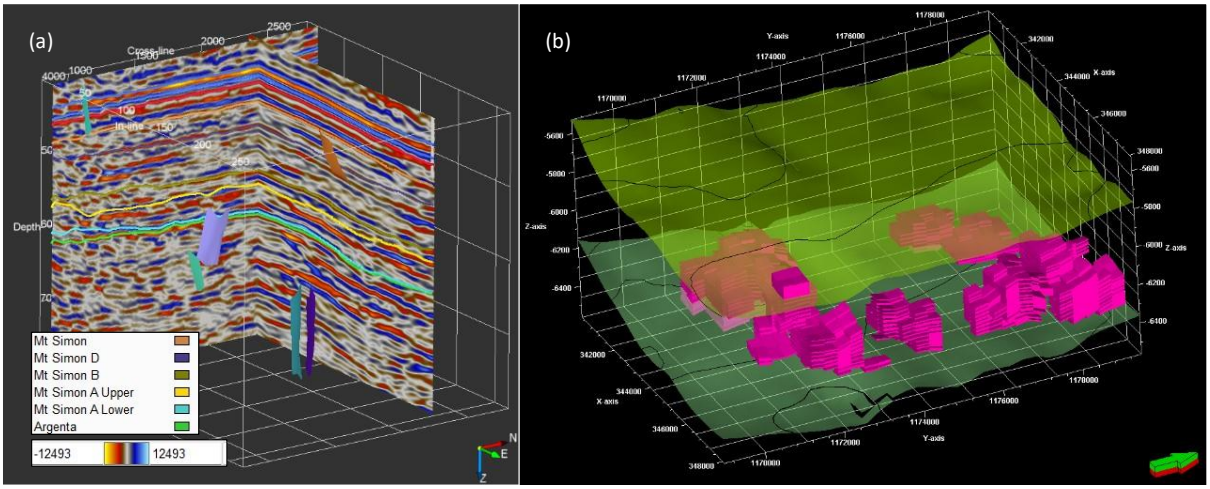

Figure 3. (a) 3D cube showing interpreted faults, horizons, and seismic data for the reservoir. (b) Interpreted geobodies within Mt. Simon B and Precambrian horizons after converting them to grid cells.

Petrophysical Analysis: K-Mean Clustering, employing NPHI, RHOB, PEF, and DTCO parameters, was conducted to discern six lithotypes, comprising three sandstones, two shale types, and one calcareous variety (Figure 4). Neutron-Density data facilitated the computation of V-Shale and Effective Porosity within the well logs, Permeability log was calculated based on the lithology and the effective porosity through a linear regression discriminating by lithology. The lithology model was refined through calibration with drill cores and RCA tests, culminating in the construction of a comprehensive lithologic facies log. Results can be seen in Figure 5.

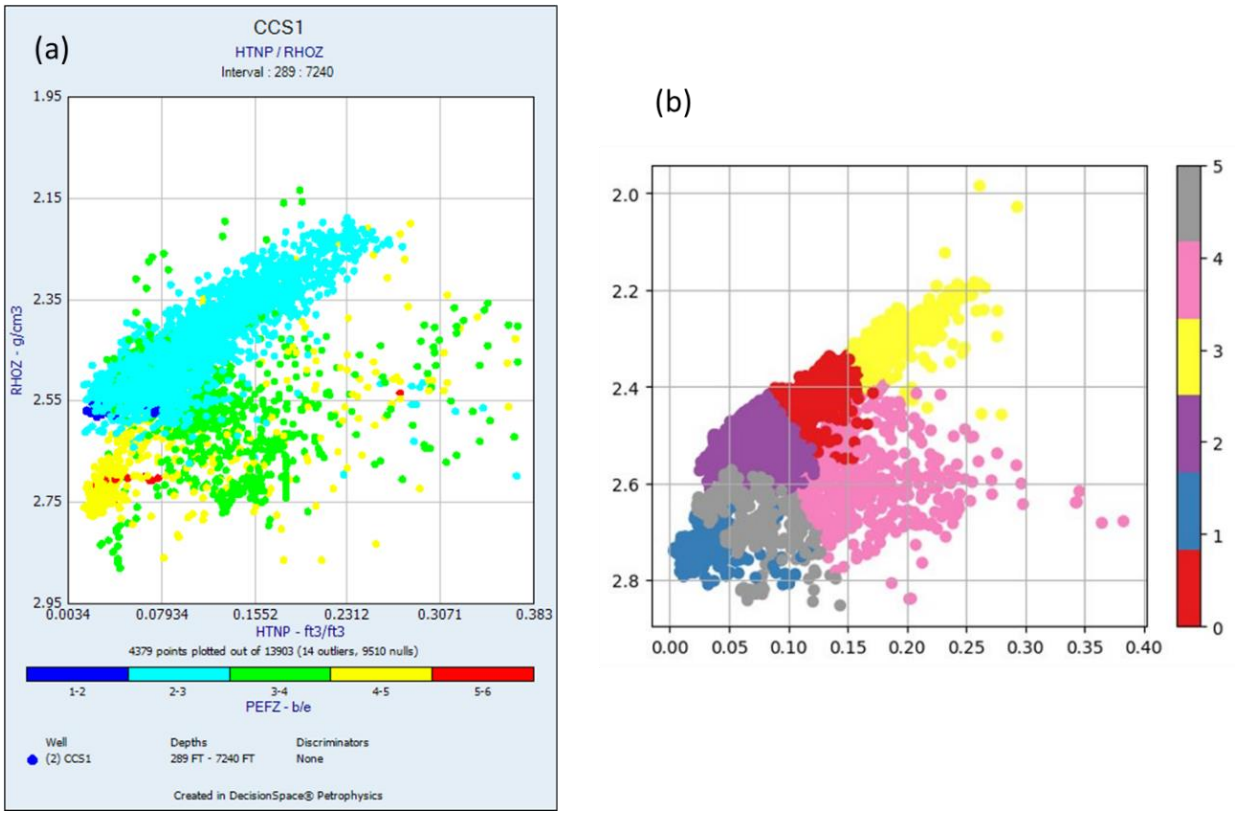

Figure 4. (a) K-Mean clustering using well logs. (b) Calculated distribution of lithotypes. The axes of the figure are RHOZ y HNTP.

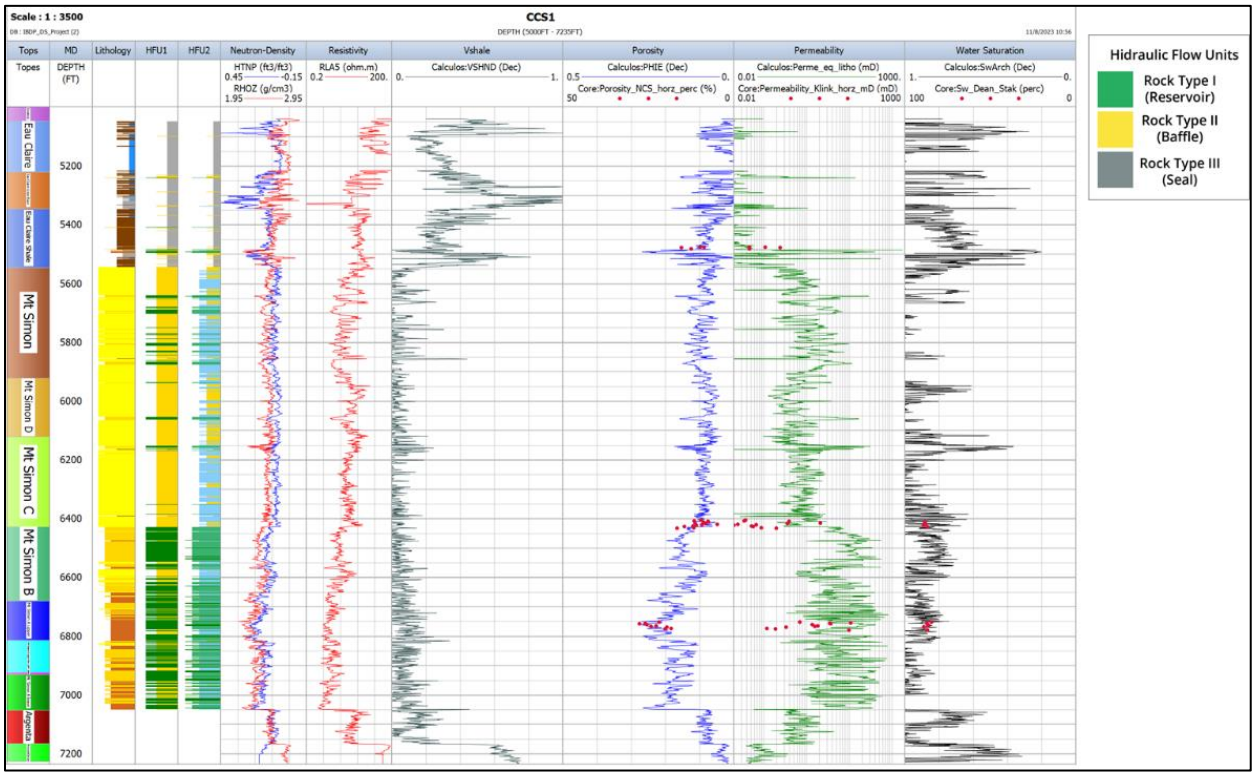

Figure 5. Well logs for CCS1, calculated V-shale, Porosity, Permeability and Hydraulic Flow Units.

Hydraulic flow units shown in Figure 5 were computed using the Winland R35 methodology (Kodozie, 1980), revealing Mt. Simon B and Mt. Simon A formations as promising targets, while the upper members of Mt. Simon were identified as potential baffle zones, the Eau Claire formation was recognized for its sealing effectiveness (Table 1). Figure 6 shows the reliability of the rock types being reservoir, baffle, and seal zones. The correlation with elastic parameters exhibited a commendable degree of accuracy, substantiating the robustness of the undertaken methodology.

HFU	Vsh	Phi	K	Sw
Rock Type 1 (Reservoir)	0.001 - 0.4512	0.1181 - 0.3670	5.2916 - 26082	0.2464 - 1
Rock Type 2 (Baffle)	0.001 - 0.5508	0.0317 - 0.1639	0.0328 5.25	0.3275 - 1
Rock Type 3 (Seal)	0.2029 - 1	0.0001 - 0.1091	0.0001 - 0.0419	0.3747 - 1

Table 1. Hydraulic Flow Units and their properties.

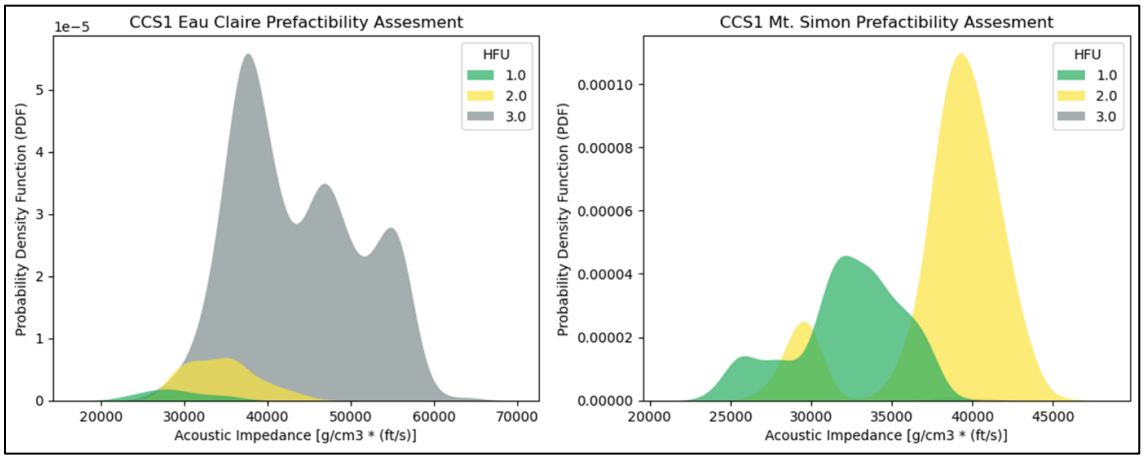

Figure 6. CCS1 Acoustic Impedance Probability Density Functions for Eau Claire and Mt. Simon, showing computed Hydraulic Flow Units for both.

Static Modeling: The static modeling process was conducted within Petrel software, using a structural grid with dimensions of 24 x 32 x 190 cells, measuring 7874 ft, 10498 ft, and 2373 ft respectively. The grid dimensions were determined based on previously interpreted seismic data, regions with unreliable resolution were systematically excluded from the grid, ensuring the fidelity and accuracy of the modeling outcomes.

Facies modeling was done using petrophysical data, well logs and defined zones based on the main horizons, which act as the model boundaries. This included the incorporation of previously defined geobodies, interpreted as bars in a fluvial depositional environment, as new facies; and the depositional trend defined by the geobodies as well (Figure 7). Porosity modeling involved the utilization of upscaled well log data and the computed facies model, employing moving average techniques for cap formations and Gaussian Simulation for the Mt. Simon formation. The methodological framework was supported by a thorough data analysis, encompassing the examination of porosity histograms and variograms for each facies, along with outlier management and the formulation of a Gaussian curve for each one. A Pore Pressure cube was done for each zone as well.

The horizontal permeability data for the model was computed through analogous methodologies, mirroring the approach employed in porosity modeling. The permeability in the vertical direction was defined as 0.4 times the horizontal permeability. A detailed 3D property cube was analyzed and discussed in the results section.

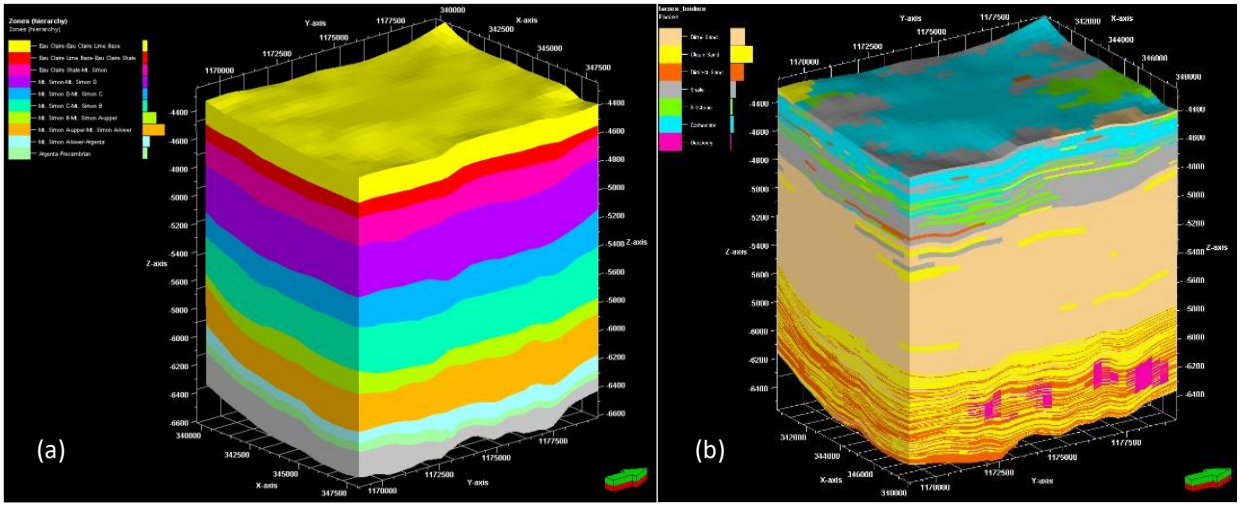

Figure 7. (a) Horizon-based zones for static modeling. (b) 3D Facies cube with geobodies (magenta colored).

Geomechanics: The geomechanical model provides information on the behavior of the rocks when subjected to the stress changes generated during any of the intervention phases, whether drilling, production, or injection. The geomechanical model was constructed using data derived primarily from the CCS1 well. Initially, key parameters were determined: vertical stress was computed from density logs, pore pressure was derived from DTCO (Differential Sonic Compressional Slowness), Dynamic Young's Modulus was calculated using resistivity logs, and Dynamic Poisson's Ratio was established based on DTSM (Differential Sonic Shear Slowness). Subsequently, horizontal stresses, fracture pressure, cohesion, internal friction angle, and collapse pressure were assessed; the equations are described in (Table 2). To ensure the model's validity, a comparison was made with the mud weight information extracted from ISGS (2023) drilling reports.

To evaluate the faults reactivation potential, the gathered information was integrated into Stanford University's freely available FSP (Fault Slip Potential) software. This step involved the incorporation of essential data on borehole stresses and faults, as previously calculated and documented in the seismic reports.

Description	Equation	Parameters	Reference
Pore pressure	$PP = s_v - (s_v - PP_n)(\frac{\Delta t_0}{\Delta t_n})^{1,2}$	s_v Vertical stress PP_n Compaction trend $\frac{\Delta t_0}{\Delta t_n}$ Porosity ratio	Novoa & Villaveces. (2013).
Minimum horizontal pressure	$\sigma_h = (\sigma_v - \beta P_p)\left[\frac{v}{(1-v)}\right] + \beta P_p$	σ_v Vertical stress β Biot constant P_p Pore pressure V Dynamic Poisson's ratio	Zhang, J. J. (2019)
Maximum horizontal pressure	$\sigma_H = 1{,}2\ \sigma_h$	σ_h Minimum horizontal pressure	Delgado y Vanessa Manrique, O. (2016).
Fracture pressure	$gPf = \frac{v}{1-v}(g_v - g_{Pp}) + g_{Pp}$	v Dynamic Poisson's ratio g_v Vertical stress g_{Pp} Pore pressure	Delgado y Vanessa Manrique, O. (2016).

Internal Friction Angle	$\theta = sin^{-1}(\frac{V_p - 1000}{V_p + 1000})$	v_p Rock Compressibility	Lal, 1999
Collapse Pressure	$Pc = \frac{(3\sigma H - \sigma h)(1 - sen\ \theta) - (C * \cos\theta) + (Pp\ sen\ \theta)}{2}$	σH Maximum horizontal pressure σh Minimum horizontal pressure θ Internal Friction Angle C Cohesion Pp Pore pressure	Delgado y Vanessa Manrique, O. (2016).

Table 2. Methodologies and correlations to build the geomechanical model.

Simulation: Through conceptual simulation models, an analysis of CO_2 trapping mechanisms was conducted in two simulation scenarios: the first in a homogeneous porous and permeable medium, and the second in a heterogeneous porous and permeable medium. The objective was to establish the behavior of the CO_2 plume in these different scenarios with homogeneous and isotropic lateral characteristics versus heterogeneous model with anisotropic lateral characteristics. This aimed to analyze the effects of permeability variations occurring in a laterally heterogeneous geological unit, as represented by the static model developed for the IBDP (see Figure 8).

Results

The static modeling process culminated in the generation of both permeability and porosity cubes, as exhibited in Figure 8. These models reveal lateral variations that are in accordance with the geobody trends previously established in the facies modeling phase, and evidence permeability and porosity increase in the zones where the geobodies are, enhancing the reservoir capacity. The effective porosity values within the modeled area range from a minimum of 0.0001 ft³/ft³ to a maximum of 0.2750 ft³/ft³. A net to gross ratio has been determined, with porosity values exceeding 0.15 ft³/ft³ considered reliable for further analysis (Figure 9). The distribution of porosity values suggests a highly heterogeneous reservoir, possibly influenced by the depositional environment, fluvial dynamics, and subsequent diagenetic processes.

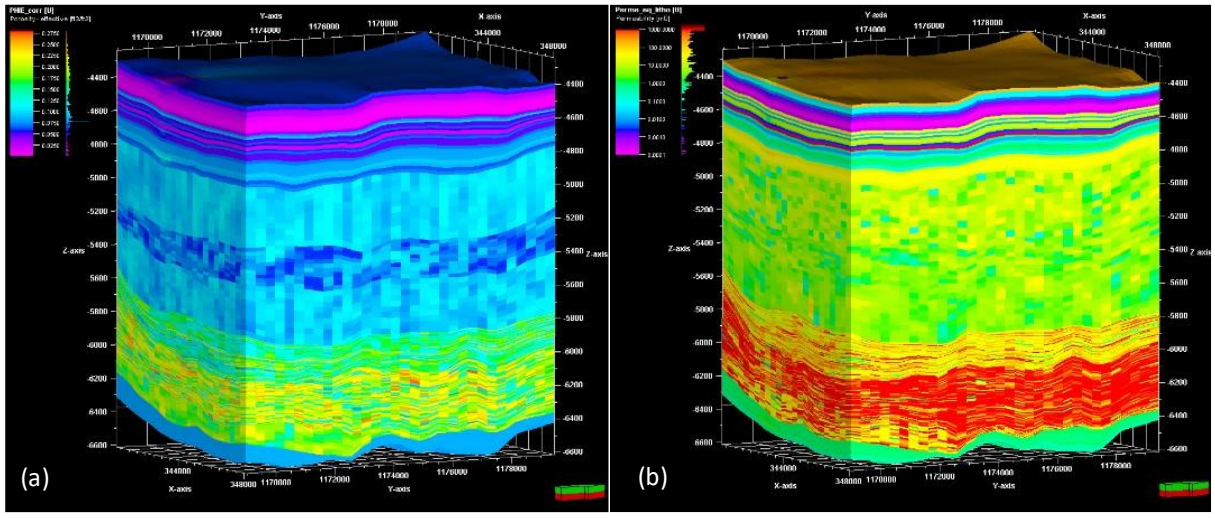

Figure 8. (a) Effective Porosity model. (b) Permeability model.

Permeability data display lateral variations, which are evidently controlled by both the geobody trends and fault structures. The maximum permeability recorded was 841.17 millidarcies (mD), measured prior to injection at well CCS1. Post-injection data from monitoring well VW1 indicated anomalously high permeability values, exceeding 200,000 mD, which have been rationalized to a ceiling value of 1000 mD

to maintain model stability and realism. The minimum permeability measured was 0.0001 mD, indicating zones of potentially negligible fluid flow.

The Eau Claire formation, acting as the seal, consistently shows low porosity and permeability values, affirming its efficacy as a barrier to fluid migration. Contrastingly, the Mt. Simon formation, particularly the Mt. Simon A and B members designated as the reservoir, exhibits higher porosity and permeability. The intermediate Mt. Simon C and D members, as well as the upper Mt. Simon, serve as baffle rocks with variable properties.

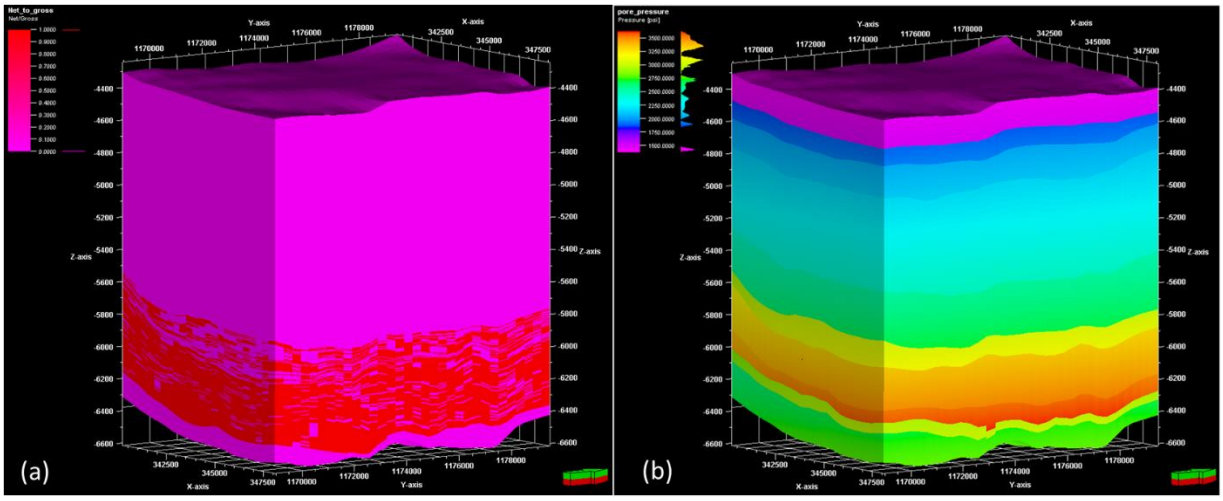

Figure 9. (a) Net-to-gross Cube, areas with higher than 0.15 ft³/ft³ porosity are red colored. (b) Average pore pressure cube.

The geomechanical model included the stress state, rock strength, and geological structure, focusing on three main components: pore pressure, horizontal and vertical maximum and minimum geomechanical stresses. This model was crucial for understanding the subsurface stress regimes and their implications for CAC (Cyclic Steam Stimulation) operations.

The model aligns with a normal stress regime, which provides reliability in determining the stability window, which we compare with the reported mud weight (Figure 10).

Six faults were identified in the areas of interest, cutting through the Mt. Simon formation; fault data is provided in Table 3.

These faults were input into the FSP software to analyze the results. The red line in Figure 11 represents the failure envelope. If the fault points are below the envelope, it means the fault is stable, and the likelihood of it becoming a flow channel is low. Therefore, the pressure value can be maintained. It is a scenario where the fault is not stressed.

Fault	Sh Gradient (Psi/ft)	SH Gradient (Psi/ft)	Sv Gradient (Psi/ft)	Pp Gradient (Psi/ft)	Internal Friction Angle	Strike (Deg)	Dip (Deg)
1	0,870	1,269	1,099	0,476	41,750	264,680	72,77
2	0,674	0,809	0,925	0,504	38,634	269,300	61,97
3	0,598	0,717	0,912	0,457	40,650	102,010	57,26
4	0,602	0,723	0,920	0,482	40,264	269,590	89,04
5	0,751	0,901	0,922	0,607	33,684	269,070	76,45
6	0,878	1,192	1,114	0,459	45,466	263,430	53,1

Table 3. Geomechanical and geometric information of the faults.

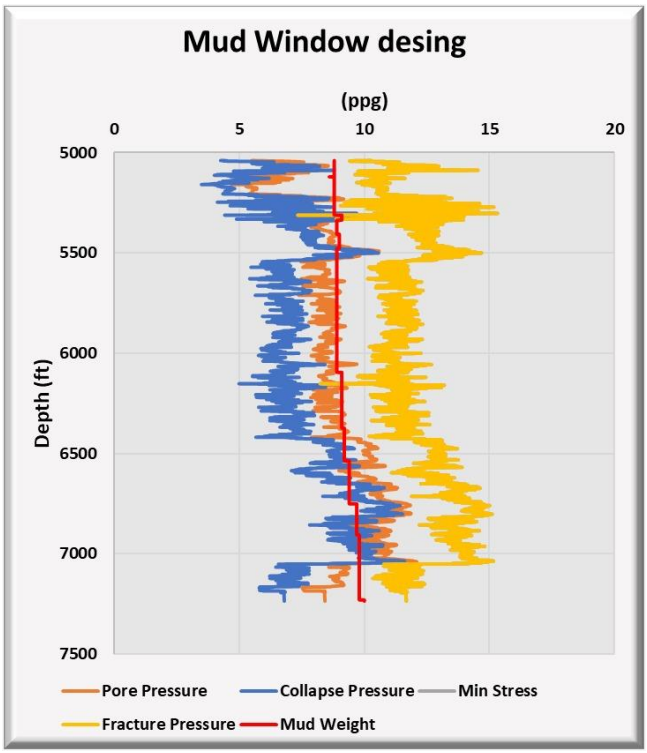

Figure 10. Safe mud window, describing the minimum pressure before fracturing. The red line shows the mud density function.

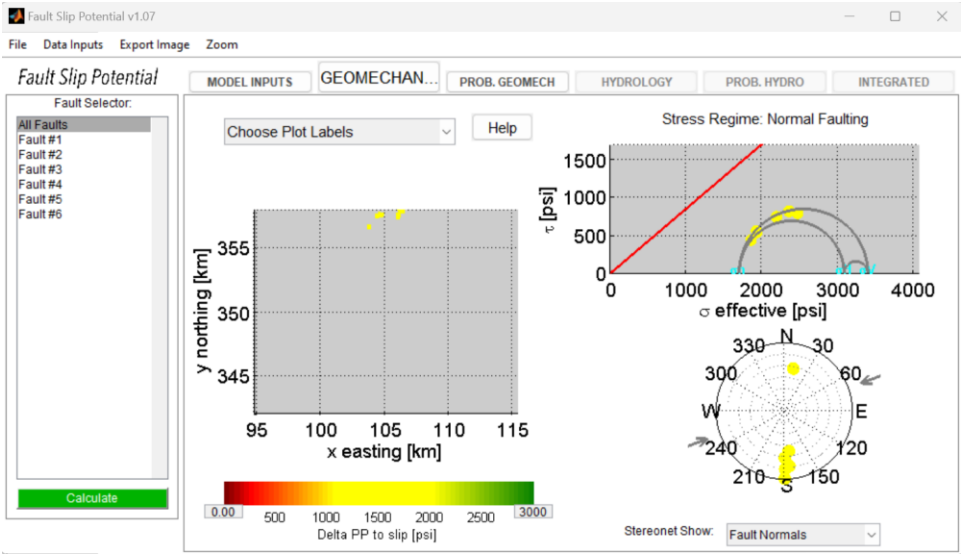

Figure 11. Results of fault reactivation potential study for the study area.

The simulation represented the injection of CO_2 from the CCS1 well, which had an injection rate of 1000 tons/day. The grid represents an area of approximately 223.5 km^2 (15 km x 14.9 km). Two simulation scenarios were developed, the first was homogenous, where the units and characteristics used for constructing the conceptual model are shown in Table 4. The involved geological units are Eu Claire: seal rock, Upper Mt Simon: baffles zone, Lower Mt Simon: area with better storage properties, and finally Argenta: transition zone between the basement and the storage rock. Average thicknesses, porosities, and permeabilities were considered (as seen in Figure 12). Petrophysical properties were extracted from the lithotypes identified in our petrophysical model.

Depth -Top (m)	Layers (8)	Grid Thickness (m)	Porosity (%)	Permeability (mD)
1630	Eu Claire	60	0.01	0.0001
1690	Mt Simon	110	0.09	2
1800	Mt Simon (D)	60	0.09	2
1860	Mt Simon (C)	100	0.2	500
1960	Mt Simon (B)	70	0.2	500
2030	Mt Simon (A) Upper	80	0.2	500
2110	Mt Simon (A) Lower	40	0.2	500
2150	Argenta	30	0.1	1

Table 4. Parameters of the conceptual simulation model

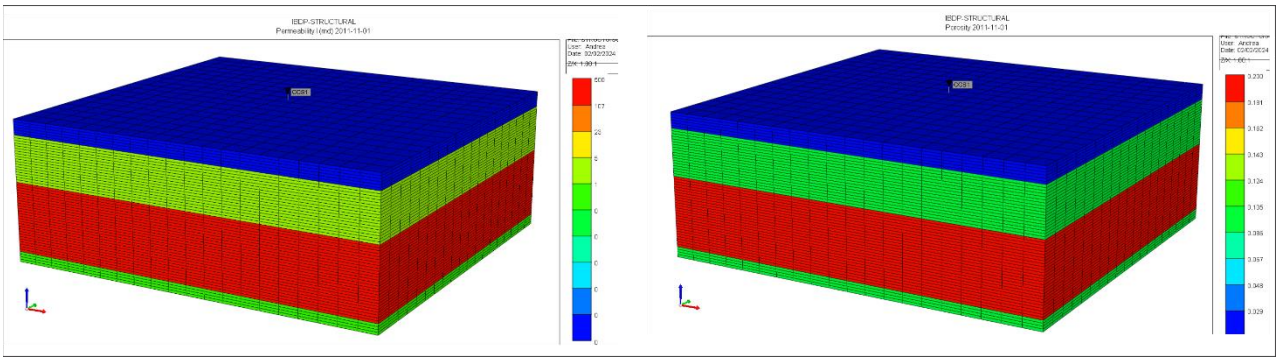

Figure 12. Petrophysical properties established in the homogeneous conceptual model, the image on the left corresponds to permeability (mD) and the one on the right corresponds to porosity (%).

In the second scenario, the simulation model was conducted using the static model built in Petrel, which was imported as a RESCUE file into the CMG software. The porosity and permeability properties represent the modeled reservoir heterogeneities, as depicted in Figure 13. Additionally, the model incorporates interpreted faults to simulate a scenario closer to IBDP conditions.

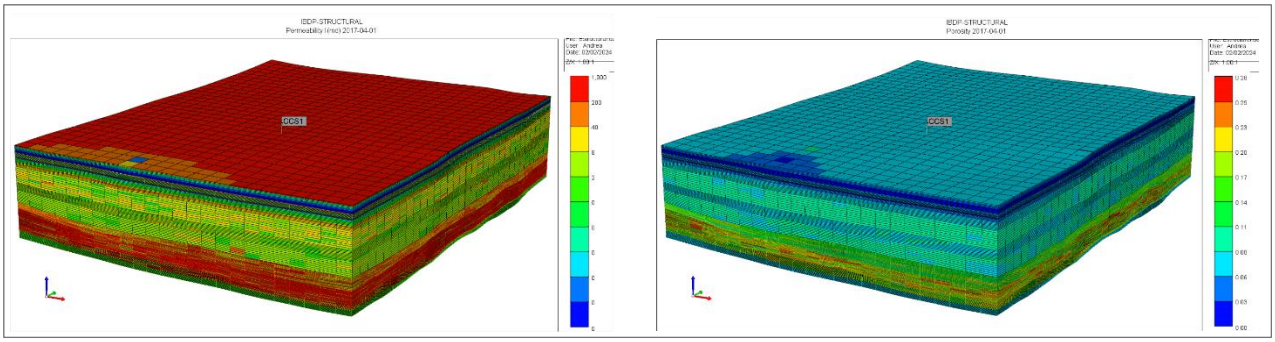

Figure 13. Petrophysical properties established in the heterogeneous realistic model, the image on the left corresponds to permeability (mD) and the one on the right corresponds to porosity (%).

For these two scenarios, the different trapping mechanisms that occur in a porous medium are evaluated: structural, hysteresis and solubility. It is expected that in the IBDP case, where CO_2 storage occurs in an aquifer, solubility is the most influential mechanism on the CO_2 storage capacity.

For the structural case, the behavior of CO_2 can be observed, which tends to migrate until it encounters the seal formation. This gas saturation behavior aligns with pressure changes, as depicted in Figure 14. In the structural trapping mechanism, it is evident that the vertical migration is slightly dispersed by the reservoir heterogeneities.

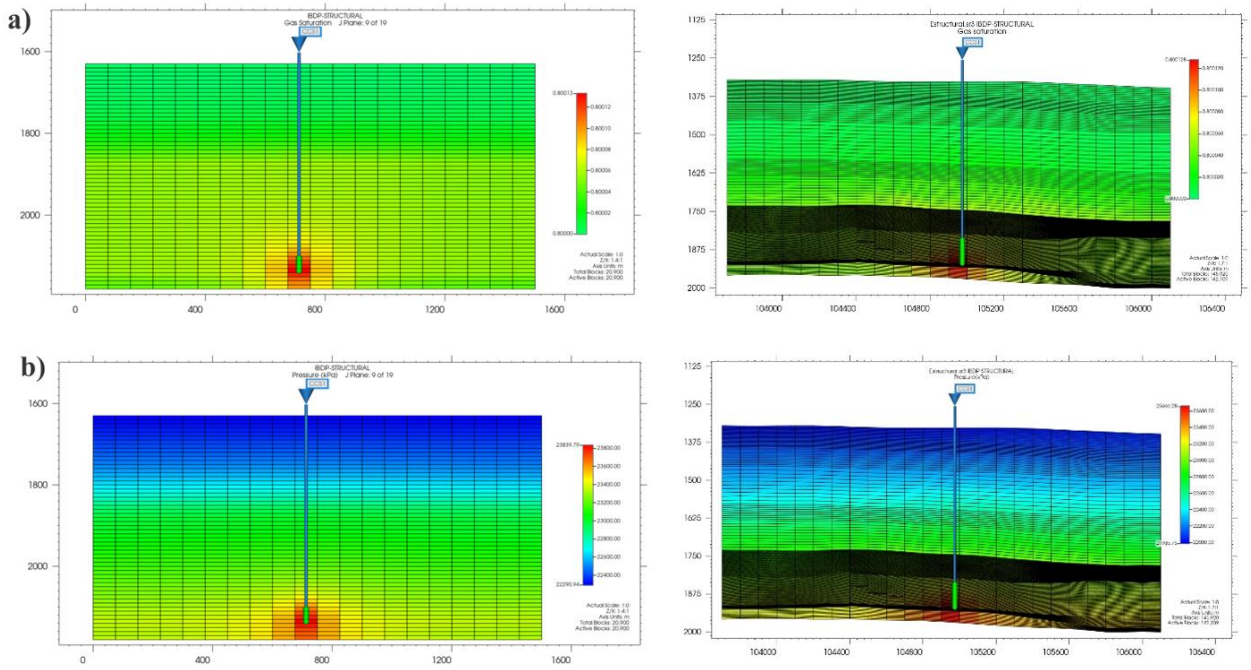

Figure 14. Distribution and behavior of the CO_2 plume due to the structural trapping mechanism. (a) Gas saturation (b) Pressure (kPa). On the left the homogeneous model, on the right the heterogeneous model.

For the hysteresis phenomenon, the behavior of the CO_2 plume is analyzed through the critical gas saturation parameter CO_2, where the trapping of CO_2 in the pore space is evident as the plume stabilizes at different time stages, first during the injection (2020) and estimated 30 years after the injection is completed (2050). Figure 15 shows that this parameter positively influences the safety of long-term storage since it guarantees the trapping of CO_2 by capillary forces. Furthermore, it is observed that the heterogeneity of the reservoir influences reducing the lateral displacement of the CO_2 plume, allowing lateral migration to decrease.

For solubility trapping, other parameters are also reviewed, such as the mole fraction of CO_2 dissolved in water. It is evident how the CO_2 concentration increases in the reservoir aquifer through the dissolution effect (Figure 16). This mechanism is also affected by the heterogeneity of the reservoir since the displacement of the plume will respond to these heterogeneities. This mechanism is considered safe, because given the chemical reactions that occur, CO_2 ceases to exist as a free phase.

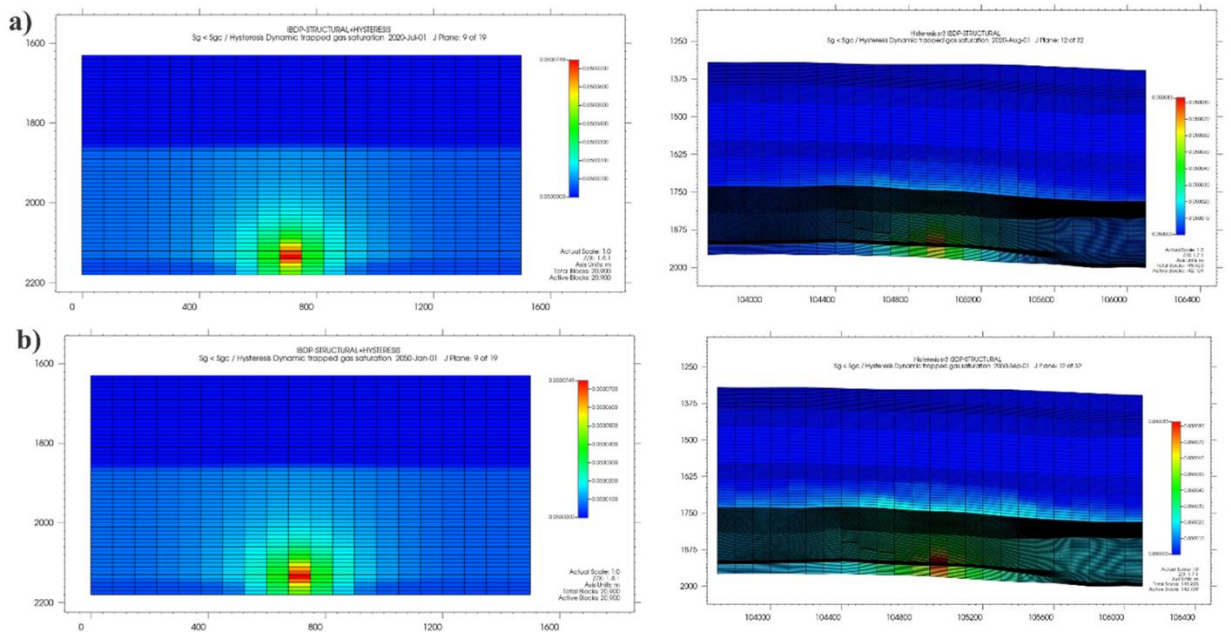

Figure 15. Distribution and behavior of the CO_2 plume due to the hysteresis phenomenon. (a) Time at which the injection stops (2020) (b) time 30 years after the injection ends (2050). On the left the homogeneous model, on the right the heterogeneous model.

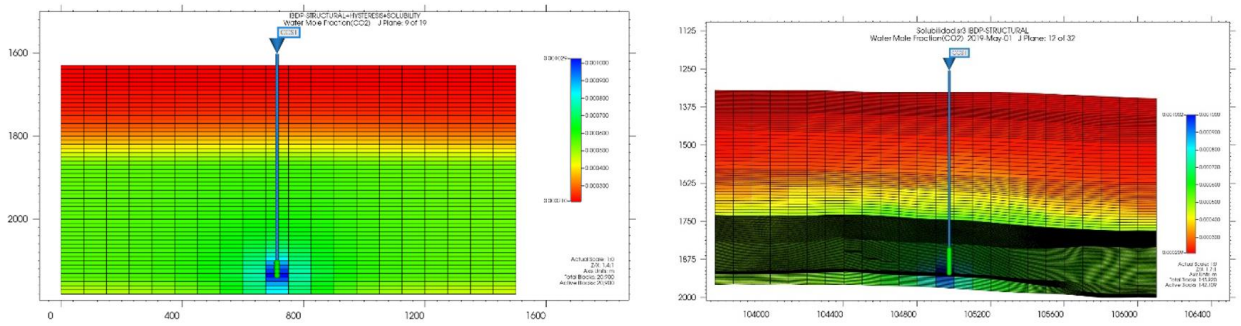

Figure 16. Distribution and behavior of the CO_2 plume due to the solubility effect. On the left the homogeneous model, on the right the heterogeneous model.

Conclusions

The Mt. Simon formation, particularly the A and B segments, have been identified as favorable reservoirs for CO_2 storage. Their petrophysical characteristics are suitable for containing substantial volumes of CO_2. The presence of geobodies and lateral accretion patterns within these segments has been found to significantly affect the CO_2 plume geometry. These characteristics have considerable implications for the storage potential, emphasizing the need for precise modeling in storage capacity prediction and injection planning.

The C and D segments serve as effective baffle zones, augmenting the seal integrity provided by the Eau Claire formation. The reliability of these baffle zones is crucial for the successful implementation of CO_2 storage strategies within the Mt. Simon formations.

Simulation, which included properties model and geomechanics, have determined a pressure variation range that is expected to maintain reservoir integrity without inducing fracturing. Additionally, the study has confirmed the stability of fault systems under simulated conditions, which is favorable for the security of CO_2 storage.

Acknowledging the heterogeneities in porosity and permeability has been essential in understanding their impact on CO_2 storage. These variations play a significant role in both structural trapping and in controlling dynamic storage processes such as hysteresis and solubility, which are important for the efficacy and safety of CO_2 sequestration.

In conclusion, the results of this study demonstrate the Mt. Simon formations' strong potential for CO_2 storage. Detailed geological characterization is crucial to effectively harness this potential and to ensure robust and secure CO_2 sequestration.

References

Bauer RA, Will R, E. Greenberg S, Whittaker SG. Illinois Basin–Decatur Project. In: Davis TL, Landrø M, Wilson M, eds. Geophysics and Geosequestration. Cambridge: Cambridge University Press; 2019:339-370. http://dx.doi.org/10.1017/9781316480724.020.

Brown, A. (2010). ADM-Update of Base Case Modeling Decatur Project. Schlumberger Carbon Services.

CHANG, C; ZOBANCK, M-& KHAKSAR, A. Empirical relations betwwn rock strength and physical properties in sedimentary rocks. In journal of pretroleum research, Vol 23 No. 3, 223-237, 2006. The Netherland Elsevier.

Delgado y Vanessa Manrique, O. (2016). Metologia para diseñar el Modelo geomecnico de estabilidad de pozo.

Freiburg, J. T. (2014). A Depositional and Diagenetic Characterization of the Mt. Simon Sandstone at the Illinois Basin - Decatur Project Carbon Capture and Storage Site, Decatur, Illinois, USA, 73.

Freiburg, J. T., McBride, J. H., Malone, D. H., & Leetaru, H. E. (2020). Petrology, geochronology, and geophysical characterization of Mesoproterozoic rocks in central Illinois, USA. Geoscience Frontiers, 11(2), 581-596.

Illinois State Geological Survey (ISGS), Illinois Basin - Decatur Project (IBDP) Well Information, April 30, 2021. Midwest Geological Sequestration Consortium (MGSC) Phase III Data Sets. DOE Cooperative Agreement No. DE-FC26-05NT42588., http://dx.doi.org/10.18141/1854144.

Zaluski, W., & Lee, S. (2020). IBDP Final Static Geological Model Development and Dynamic Modelling. SLB, US Department of Energy, National Energy Technology Laboratory. https://edx.netl.doe.gov/dataset/598a5157-de71-4360-b4ba-5fc0f98982ae/resource/d9c5f1cf-445a-44e3-8f06-7ab74ab36a7c.

Illinois State Geological Survey, US Department of Energy, Archer Daniels Midland Company, Schlumberger, & Trimeric Corporation. (2023). Illinois Basin - Decatur Project Dataset. http://dx.doi.org/10.11582/2022.00017.

Kolodzie Jr., S. (1980). Analysis Of Pore Throat Size and Use of The Waxman-Smits Equation to Determine Ooip in Spindle Field, Colorado. https://doi.org/10.2118/9382-MS

Leetaru, H. E., & Freiburg, J. T. (2014). Litho-facies and reservoir characterization of the Mt Simon Sandstone at the Illinois Basin - Decatur Project. Greenhouse Gases: Science and Technology, 4(5), 580–595. http://dx.doi.org/doi:10.1002/ghg.1453.

Novoa y Diego Raul Villaveces Suares, P. F. Q. (2013). Determinacion de la mejor trayectoria de perforación basada en una analisis geomecanico, aplicado al campo escuela colorado.

Swann, D. H. (1968). A summary geologic history of the Illinois Basin. Geology and Petroleum Production of the Illinois Basin, 3-21.

Weller, J. M., & Bell, A. H. (1937). Illinois basin. AAPG Bulletin, 21(6), 771-788.

Zaluski, W., & Lee, S. (2020). IBDP Final Static Geological Model Development and Dynamic Modelling. SLB, US Department of Energy, National Energy Technology Laboratory. https://edx.netl.doe.gov/dataset/598a5157-de71-4360-b4ba-5fc0f98982ae/resource/d9c5f1cf-445a-44e3-8f06-7ab74ab36a7c.

Zhang, J.J. (2019) Rock Physical and Mechanical Properties.